A pixel-by-pixel equalization method for the X-ray imaging polarimeter on board the IXPE mission

John Rankin[a], Fabio Muleri[a], Enrico Costa[a], Alessandro Di Marco[a], Sergio Fabiani[a], Fabio La Monaca[a], Paolo Soffitta[a], Luca Baldini[b], Alberto Manfreda[c], Stephen L. O'Dell[d], Matteo Perri[e], Simonetta Puccetti[f], Brian D. Ramsey[d], Carmelo Sgrò[c], Allyn F. Tennant[d], and Martin C. Weisskopf[d]

[a]INAF - Istituto di Astrofisica e Planetologia Spaziali (Italy)
[b]Univ. di Pisa (Italy)
[c]Istituto Nazionale di Fisica Nucleare (Italy)
[d]NASA Marshall Space Flight Ctr. (United States)
[e]INAF - Osservatorio Astronomico di Roma (Italy)
[f]Agenzia Spaziale Italiana (Italy)

ABSTRACT

On December 9, 2021, the Imaging X-ray Polarimetry Explorer (IXPE) observatory was launched, carrying three X-ray polarimeters based upon the Gas Pixel Detector (GPD). These devices measure the photoelectron's ionization track following absorption of an X-ray, from which the photoelectron's initial direction (correlated to the polarization position angle) is determined. Here we describe a method for event-by-event correction of pixel-by-pixel gain variations, which are found to be +/-20%, by comparing the charge in each pixel with the average at the same relative position inside tracks of the same shape. Using the large dataset acquired during on-ground calibration of the IXPE detectors, we have individually calibrated each of the 300x352 pixels of each detector's ASIC. We discuss the performance improvements obtained using this method, which may be relevant to other instruments that detect individual events through images.

Keywords: X-ray polarimetry, gas pixel detectors, X-ray Astronomy, Pixel Calibration

1. INTRODUCTION

The Imaging X-ray Polarimetry Explorer (IXPE) mission[1,2] is the first observatory dedicated to X-ray polarimetry. It carries on board three X-ray optics modules and three X-ray polarization sensitive detectors[3] based on the Gas Pixel Detector (GPD[4–6]). This detector has previously also flown on the PolarLight mission[7] and will also fly on future missions such as eXTP.[8]

The GPD is a detector, based on the photoelectric effect, sensitive to the polarization of X-rays. A schematic of it is shown in figure 1. An incident X-ray enters through the beryllium window and its absorption causes the formation of a photoionization track in the DME gas inside the cell. In the detector there is a drift field, which causes the charge to move towards the Gas Electron Multiplier, were it is multiplied. The charge is then collected by a custom ASIC, specifically developed for X-ray polarimetry,[5] producing the image of the photoelectric track. The distribution of the directions of these tracks peaks along the direction of polarization, while the amplitude of the modulation of this distribution is proportional to the polarization degree. Therefore, to compute the polarization of incident radiation, we need to determine the direction of these ionization tracks. We do this using a reconstruction algorithm based on the charge distributions of the image. Under development is also a track reconstruction technique based on neural networks.[9]

Because the track direction contains all the polarization information, its shape needs to be accurately imaged by the pixels of the ASIC, requiring systematic effects to be as small as possible. This is particularly complex

Further author information: (Send correspondence to John Rankin)
John Rankin: E-mail: john.rankin@inaf.it

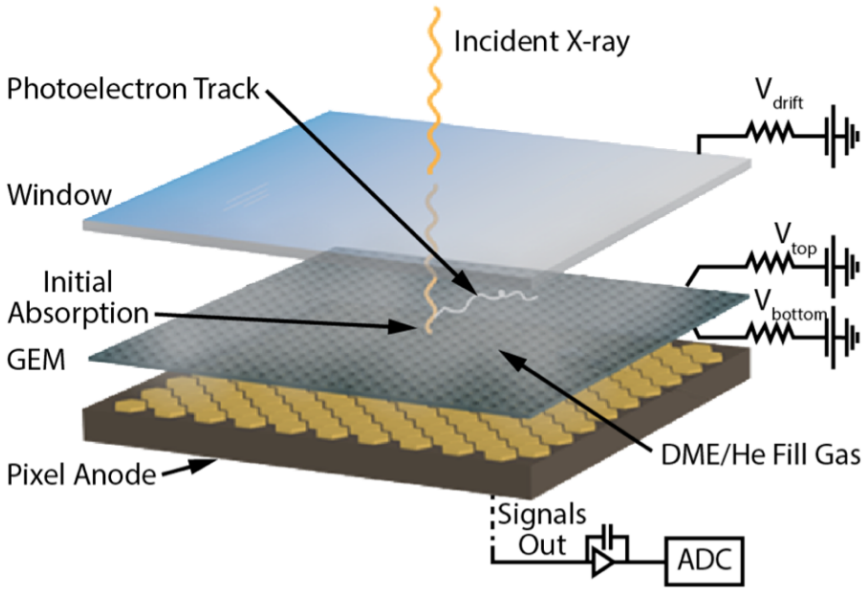

Figure 1. Schematic of the GPD. See the text for details. Image credit: Ref. 11

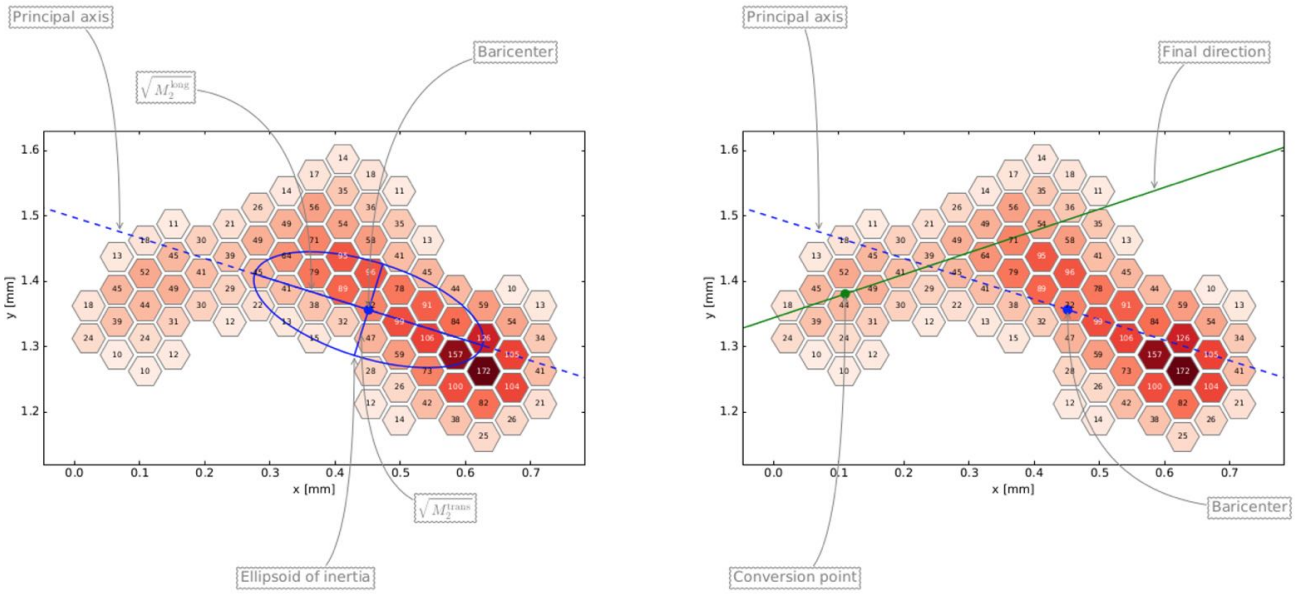

Figure 2. Example of a photoelectric track on the GPD. The part in darker color, with the greatest charge density (the Bragg peak), is the one formed last. The part with less charge is the one containing the real polarimetric information. The reconstruction algorithm used to determine polarization (Ref. 10) identifies the Bragg peak first (left side of the figure) and then reconstructs the original direction (right side of the figure).

because Rutherford scattering causes the track direction to vary during track formation; moreover, the track is diffused before collection. The example track image in figure 2 shows this. It should be noted that the part with the greatest charge density (the Bragg peak) actually forms last, while the part with the real polarimetric information forms first and has got less charge. For this reason the reconstruction algorithm that is used to determine polarization[10] actually identifies the Bragg peak first and only at the second step reconstructs the original direction.

As it is common in detectors made of pixels, the different pixels have a different gain. This causes dis-

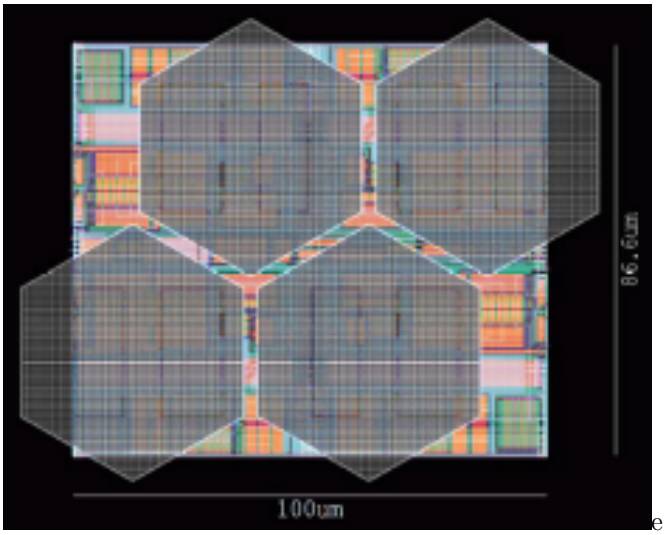

Figure 3. All pixels are collected in basic units of 4 pixels, called miniclusters,ywhich are logically OR-ed together. The reference system is such that the top-left pixel in the minicluster has always both coordinates even. Image credit: Ref. 5

uniformities in the image which can change the reconstructed direction of all the ionization tracks, potentially introducing a systematic effect in the measured polarization, and unfortunately the GPD ASIC doesn't have an electronic calibration system which is reliable to the needed accuracy.

To produce a uniform track image, pixel by pixel gain variations have to be equalized. Here we describe the application of a method that, as a by-product of ground calibration measurements, performs this equalization. The method requires calibration measurements with great statistics, which were acquired for IXPE ground calibration; nevertheless, the method can be applied to other detectors producing images of tracks.

2. THE TRACK READOUT OF THE GAS PIXEL DETECTOR

The ASIC is made of 300×352 hexagonal pixels. All pixels are collected in basic 2×2 units of pixels, called miniclusters. The four pixels are logically OR-ed together (figure 3), and have their own output chain.

The role of the minicluster is to issue a trigger when the collective signal from the four pixels exceeds a certain threshold, which can be adjusted for each minicluster. As the charge density of the photoelectron track is higher at the Bragg peak, the miniclusters usually triggers in the end part of the track. For this reason, when an event occurs, the pixels read are those from a region called *Region Of Interest (ROI)*, which is composed of the miniclusters that triggered, plus 8 pixels (4 miniclusters) along the x direction and 10 pixels (5 miniclusters) along the y direction. The reason for the discrepancy between the two axes is to compensate the fact that each minicluster has not a square shape but, due to the hexagonal shape of the pixels, the width is greater than the height.

An example acquisition with many different tracks and corresponding ROIs, over the entire surface of the ASIC, is shown in figure 4.

3. PIXEL BY PIXEL EQUALIZATION METHOD

From the number and position of the miniclusters that trigger for each event, a ROI identified with a specific size and position is read-out. Each pixel inside such a ROI collects a different charge in different ROIs, dependent on its gain and its relative position inside the ROI.

These differences in charge, due to the different pixel positions in a specific ROI, disappear when averaging many ROIs with the same specific shape. This allows to decouple the effect of gain from that of position, making it possible to compare the gain of a pixel with the average one, obtained from averaging the ROIs over the entire surface.

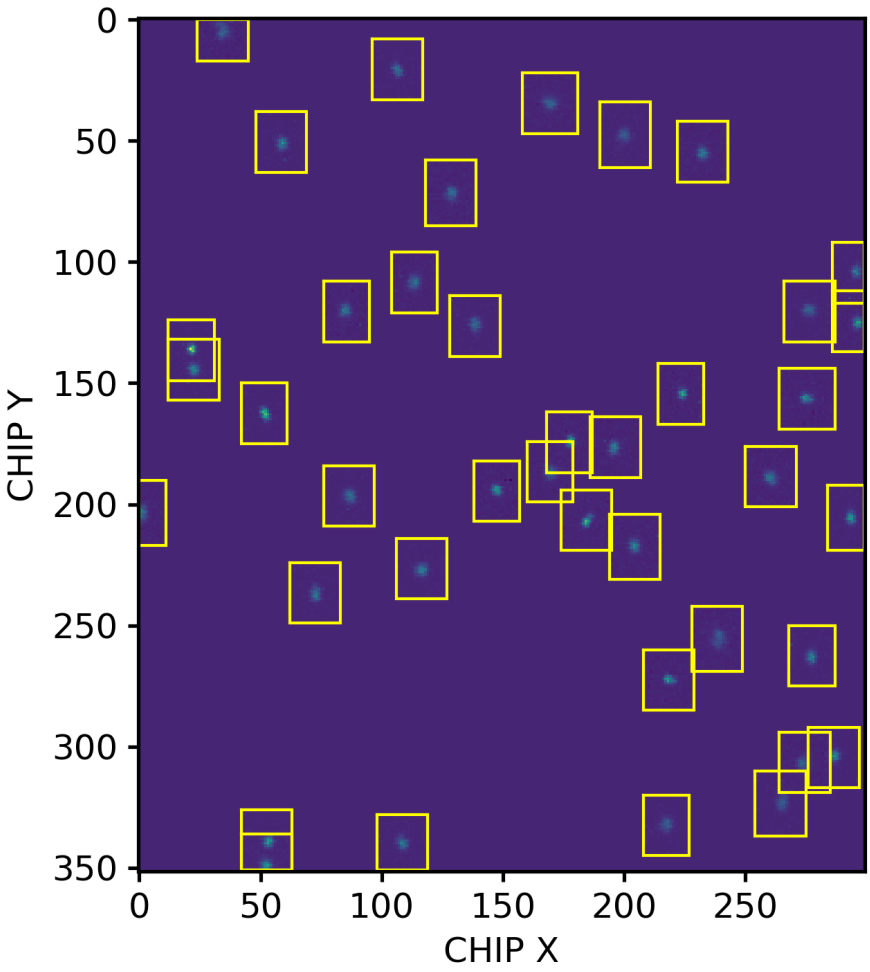

Figure 4. Example acquisition with many different tracks and corresponding ROIs over the entire surface of the ASIC.

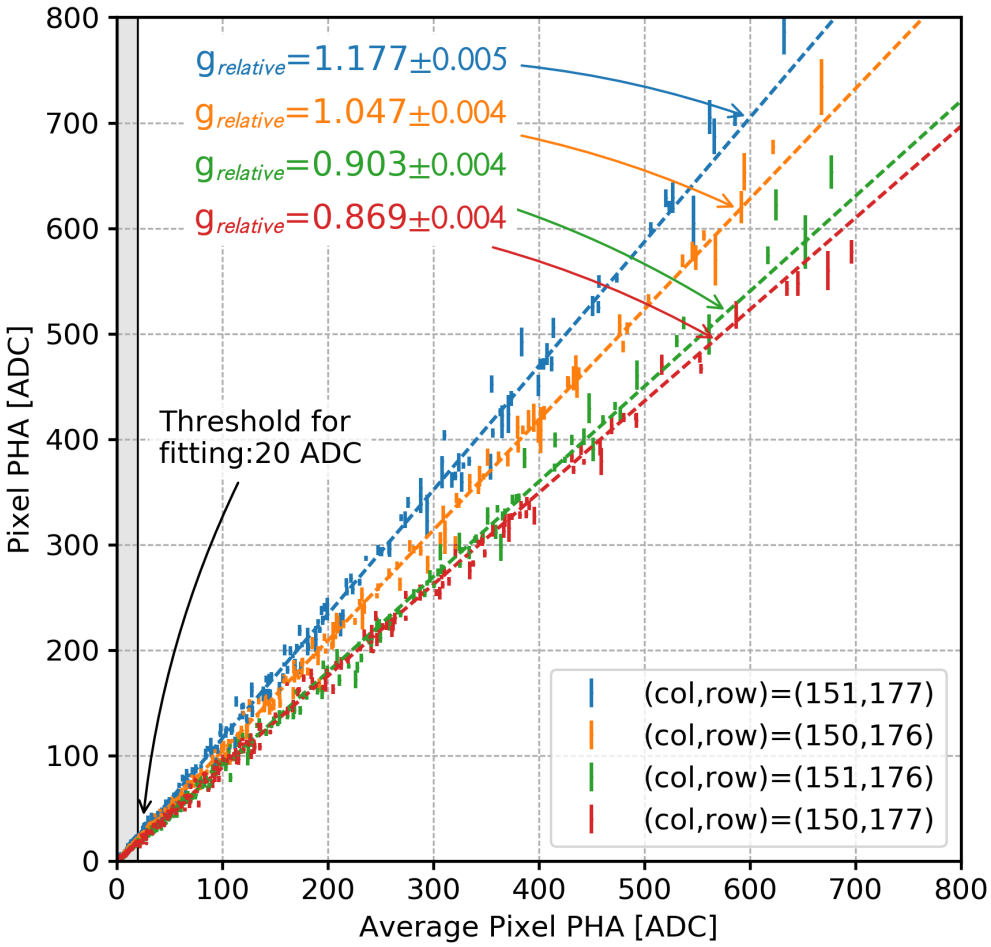

Figure 5. Pixel response by comparing the charge in different ROIs at the same absolute position with the average charge at the same relative position in the ROI. The response for four contiguous pixels is shown: the variations are significant.

As a first step in the equalization method we average ROIs of the same shape and at the same position. This gives us an image for each ROI (defined based on its start and end pixel positions in both the x and y axis). We then average ROIs of the same shape, but at different positions, to also obtain the average ROIs.

The method is based on the comparison, for each pixel, of these two kinds of averages. Figure 5 shows an example; we compare the "pixel response" defined as follows:

- The value on the y axis is the charge of the pixel in different ROIs, therefore at different relative positions inside the ROIs, but at the same absolute position on the ASIC.
- The value on the x axis is the average charge at each relative position in each ROI. This is obtained by averaging all ROIs of the same shape (in different positions on the detector)

4. TESTING THE METHOD

We tested the effects of the application of the equalization using the calibration data[12–14] acquired on ground to study the response of the detector to polarized and unpolarized radiation. Each measurement was repeated two

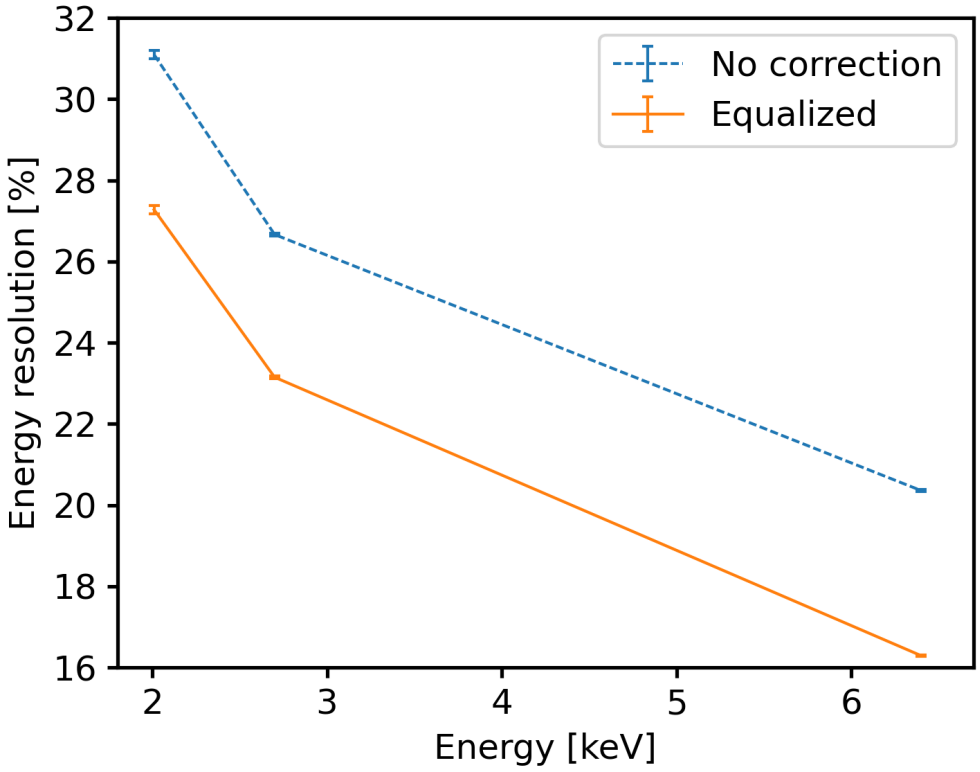

Figure 6. Energy resolution, as a function of energy, in a 0.5 mm radius spot at the center of the detector, computed without and with the application of pixel equalization. The measurements used for this plot are the polarized calibration measurements for IXPE detector 2.

times at two orthogonal angles, so to decouple the intrinsic response of the instrument to unpolarized radiation and measure the source polarization.[15] The calibrations were identical for all detector units. In the following, we will show data taken from the calibrations of IXPE detector unit number 2.

We first tested the application of the equalization by looking at how the energy resolution of the detector changes. The charge of each event measured by the GPD is the sum of the charges of all the track pixels. It is converted to energy using monochromatic calibration measurements at specific energies. The energy resolution is computed as the ratio of the FWHM of the spectral line over the energy. For this task we used the polarized radiation measurements.[16] Such measurements are obtained through Bragg diffraction, and are therefore not only polarized but also monochromatic.

In figure 6 we show the energy resolution as a function of energy, using events in a 0.5 mm radius spot at the center of the detector. As expected, there is an improvement when applying the pixel equalization, which increases with energy as in this case tracks involve more pixels.

We also studied how the response of the detector to polarized and unpolarized radiation changes after applying the equalization. Pixel equalization is expected to improve the reconstruction (and therefore the polarization direction) of the single track.

The modulation factor is the response of the detector to 100% polarized radiation, and it is the factor over which the modulation must be divided to obtain the polarization. Figure 7 shows the modulation factor both with and without the application of pixel equalization. It shows some improvements when applying the pixel equalization, but only at high energies. This is expected because pixel equalization impacts the polarization direction of the single track, but such variations are casual, and so tend to be averaged over a large area which

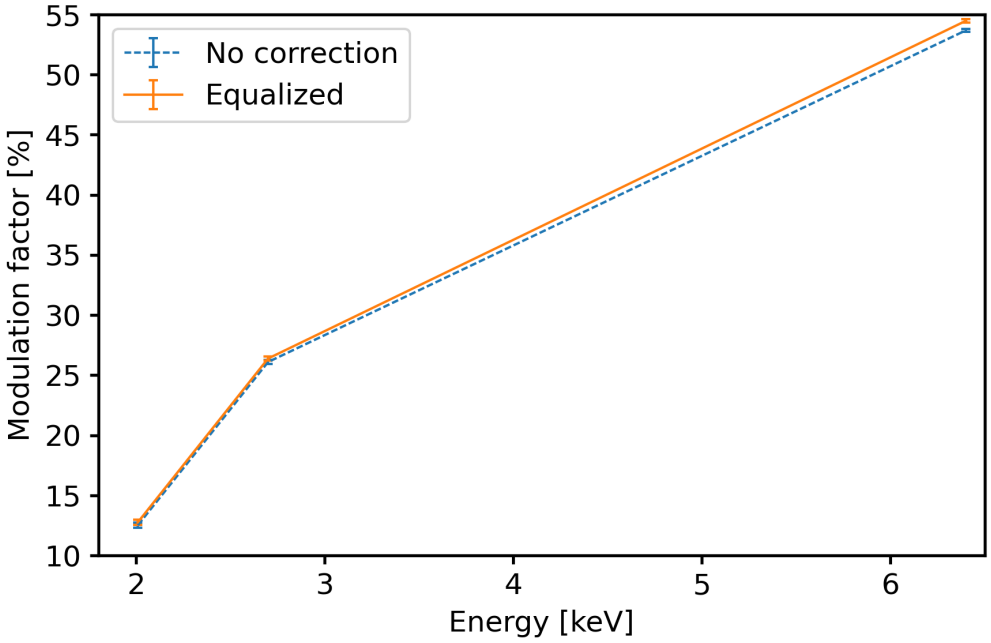

Figure 7. Modulation factor as a function of energy, in a 3 mm radius circular region at the center of the detector. Significant improvements are visible only at high energy, where tracks are more elongated.

comprises many pixels. High energy tracks are larger and more elongated, so at high energies the improvement becomes significant.

Spurious modulation is the response of the detector to unpolarized radiation, which is given only by statistics in an ideal detector, but in reality shows systematic effects which mimic a genuine signal. Figure 8 shows spurious modulation both with and without the application of pixel equalization. A significant improvement is visible at low energy, indicating that pixel equalization, by correcting the directions of the tracks, is reducing this systematic effect. The improvement is not visible at high energy because spurious modulation is negligible at high energy.

5. CONCLUSION

The Gas Pixel Detector measures the polarization of X-rays through the direction of their photoelectric ionization tracks, which are imaged by an ASIC. A thorough calibration therefore requires that pixel by pixel gain variations are equalized. A method to do this was described.

This method is based on the fact that, when an event occurs, only the part of the ASIC that contains the track is read, defining a region of interest. The method consists in the comparison of the charge of a pixel in respect to its mean value in the relative position inside all trigger regions with the same shape. The relation between the two values can be fitted with a linear function, which is then used to calibrate the pixel response of IXPE, improving its performance.

We tested the method by showing that, after applying the equalization, the energy resolution improves significantly. The response to polarization also improves, indicating that the direction of photoelectric tracks is determined more accurately, in particular for the more elongated tracks at high energies, and systematic effects in modulation are decreased.

This method could be of interest also for other instruments that, like the GPD, detect individual events through images.

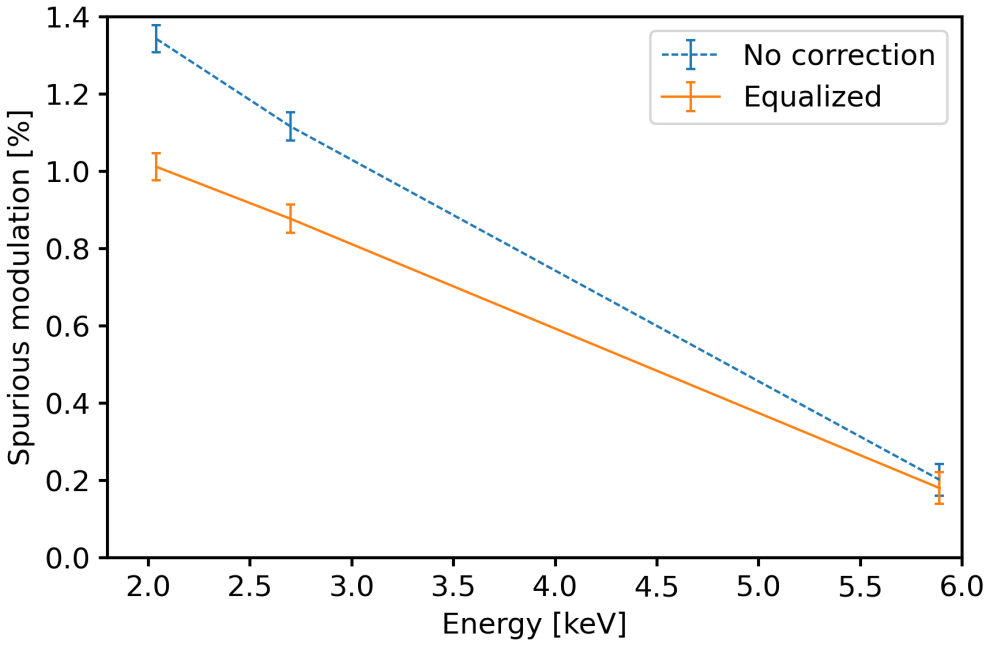

Figure 8. Spurious modulation as a function of energy, in a 3 mm radius circular region at the center of the detector.

ACKNOWLEDGMENTS

The Imaging X-ray Polarimetry Explorer (IXPE) is a joint US and Italian mission. The US contribution is supported by the National Aeronautics and Space Administration (NASA) and led and managed by its Marshall Space Flight Center (MSFC), with industry partner Ball Aerospace (contract NNM15AA18C). The Italian contribution is supported by the Italian Space Agency (Agenzia Spaziale Italiana, ASI) through contract ASI-OHBI-2017-12-I.0, agreements ASI-INAF-2017-12-H0 and ASI-INFN-2017.13-H0, and its Space Science Data Center (SSDC), and by the Istituto Nazionale di Astrofisica (INAF) and the Istituto Nazionale di Fisica Nucleare (INFN) in Italy.

REFERENCES

[1] Weisskopf, M. C., Soffitta, P., Baldini, L., Ramsey, B. D., O'Dell, S. L., Romani, R. W., Matt, G., Deininger, W. D., Baumgartner, W. H., Bellazzini, R., Costa, E., Kolodziejczak, J. J., Latronico, L., Marshall, H. L., Muleri, F., Bongiorno, S. D., Tennant, A., Bucciantini, N., Dovciak, M., Marin, F., Marscher, A., Poutanen, J., Slane, P., Turolla, R., Kalinowski, W., Di Marco, A., Fabiani, S., Minuti, M., La Monaca, F., Pinchera, M., Rankin, J., Sgro', C., Trois, A., Xie, F., Alexander, C., Allen, D. Z., Amici, F., Andersen, J., Antonelli, A., Antoniak, S., Attina', P., Barbanera, M., Bachetti, M., Baggett, R. M., Bladt, J., Brez, A., Bonino, R., Boree, C., Borotto, F., Breeding, S., Brienza, D., Bygott, H. K., Caporale, C., Cardelli, C., Carpentiero, R., Castellano, S., Castronuovo, M., Cavalli, L., Cavazzuti, E., Ceccanti, M., Centrone, M., Citraro, S., D' Amico, F., D'Alba, E., Di Gesu, L., Del Monte, E., Dietz, K. L., Di Lalla, N., Di Persio, G., Dolan, D., Donnarumma, I., Evangelista, Y., Ferrant, K., Ferrazzoli, R., Ferrie, M., Footdale, J., Forsyth, B., Foster, M., Garelick, B., Gunji, S., Gurnee, E., Head, M., Hibbard, G., Johnson, S., Kelly, E., Kilaru, K., Lefevre, C., Le Roy, S., Loffredo, P., Lorenzi, P., Lucchesi, L., Maddox, T., Magazzu, G., Maldera, S., Manfreda, A., Mangraviti, E., Marengo, M., Marrocchesi, A., Massaro, F., Mauger, D., McCracken, J., McEachen, M., Mize, R., Mereu, P., Mitchell, S., Mitsuishi, I., Morbidini, A., Mosti, F., Nasimi, H., Negri, B., Negro, M., Nguyen, T., Nitschke, I., Nuti, A., Onizuka, M., Oppedisano, C., Orsini, L., Osborne, D., Pacheco, R., Paggi, A., Painter, W., Pavelitz, S. D., Pentz, C., Piazzolla, R., Perri, M., Pesce-Rollins, M., Peterson, C., Pilia, M., Profeti, A., Puccetti, S., Ranganathan, J., Ratheesh, A., Reedy, L., Root, N., Rubini, A.,

Ruswick, S., Sanchez, J., Sarra, P., Santoli, F., Scalise, E., Sciortino, A., Schroeder, C., Seek, T., Sosdian, K., Spandre, G., Speegle, C. O., Tamagawa, T., Tardiola, M., Tobia, A., Thomas, N. E., Valerie, R., Vimercati, M., Walden, A. L., Weddendorf, B., Wedmore, J., Welch, D., Zanetti, D., and Zanetti, F., "Imaging X-ray Polarimetry Explorer: prelaunch," *Journal of Astronomical Telescopes, Instruments, and Systems* **8**(2), 1 – 28 (2022).

[2] Soffitta, P., Baldini, L., Bellazzini, R., Costa, E., Latronico, L., Muleri, F., Del Monte, E., Fabiani, S., Minuti, M., Pinchera, M., Sgro', C., Spandre, G., Trois, A., Amici, F., Andersson, H., Attina', P., Bachetti, M., Barbanera, M., Borotto, F., Brez, A., Brienza, D., Caporale, C., Cardelli, C., Carpentiero, R., Castellano, S., Castronuovo, M., Cavalli, L., Cavazzuti, E., Ceccanti, M., Centrone, M., Ciprini, S., Citraro, S., D'Amico, F., D'Alba, E., Di Cosimo, S., Di Lalla, N., Di Marco, A., Di Persio, G., Donnarumma, I., Evangelista, Y., Ferrazzoli, R., Hayato, A., Kitaguchi, T., La Monaca, F., Lefevre, C., Loffredo, P., Lorenzi, P., Lucchesi, L., Magazzu, C., Maldera, S., Manfreda, A., Mangraviti, E., Marengo, M., Matt, G., Mereu, P., Morbidini, A., Mosti, F., Nakano, T., Nasimi, H., Negri, B., Nenonen, S., Nuti, A., Orsini, L., Perri, M., Pesce-Rollins, M., Piazzolla, R., Pilia, M., Profeti, A., Puccetti, S., Rankin, J., Ratheesh, A., Rubini, A., Santoli, F., Sarra, P., Scalise, E., Sciortino, A., Tamagawa, T., Tardiola, M., Tobia, A., Vimercati, M., and Xie, F., "The Instrument of the Imaging X-Ray Polarimetry Explorer," AJ **162**, 208 (Nov. 2021).

[3] Baldini, L., Barbanera, M., Bellazzini, R., Bonino, R., Borotto, F., Brez, A., Caporale, C., Cardelli, C., Castellano, S., Ceccanti, M., Citraro, S., Di Lalla, N., Latronico, L., Lucchesi, L., Magazzù, C., Magazzù, G., Maldera, S., Manfreda, A., Marengo, M., Marrocchesi, A., Mereu, P., Minuti, M., Mosti, F., Nasimi, H., Nuti, A., Oppedisano, C., Orsini, L., Pesce-Rollins, M., Pinchera, M., Profeti, A., Sgrò, C., Spandre, G., Tardiola, M., Zanetti, D., Amici, F., Andersson, H., Attinà, P., Bachetti, M., Baumgartner, W., Brienza, D., Carpentiero, R., Castronuovo, M., Cavalli, L., Cavazzuti, E., Centrone, M., Costa, E., D'Alba, E., D'Amico, F., Del Monte, E., Di Cosimo, S., Di Marco, A., Di Persio, G., Donnarumma, I., Evangelista, Y., Fabiani, S., Ferrazzoli, R., Kitaguchi, T., La Monaca, F., Lefevre, C., Loffredo, P., Lorenzi, P., Mangraviti, E., Matt, G., Meilahti, T., Morbidini, A., Muleri, F., Nakano, T., Negri, B., Nenonen, S., O'Dell, S. L., Perri, M., Piazzolla, R., Pieraccini, S., Pilia, M., Puccetti, S., Ramsey, B. D., Rankin, J., Ratheesh, A., Rubini, A., Santoli, F., Sarra, P., Scalise, E., Sciortino, A., Soffitta, P., Tamagawa, T., Tennant, A. F., Tobia, A., Trois, A., Uchiyama, K., Vimercati, M., Weisskopf, M. C., Xie, F., Zanetti, F., and Zhou, Y., "Design, construction, and test of the Gas Pixel Detectors for the IXPE mission," *Astroparticle Physics* **133**, 102628 (Dec. 2021).

[4] Costa, E., Soffitta, P., Bellazzini, R., Brez, A., Lumb, N., and Spandre, G., "An efficient photoelectric X-ray polarimeter for the study of black holes and neutron stars," Nature **411**, 662–665 (Jun 2001).

[5] Bellazzini, R., Spandre, G., Minuti, M., Baldini, L., Brez, A., Cavalca, F., Latronico, L., Omodei, N., Massai, M. M., Sgro', C., Costa, E., Soffitta, P., Krummenacher, F., and de Oliveira, R., "Direct reading of charge multipliers with a self-triggering CMOS analog chip with 105 k pixels at 50 μm pitch," *Nuclear Instruments and Methods in Physics Research A* **566**, 552–562 (Oct. 2006).

[6] Bellazzini, R., Spandre, G., Minuti, M., Baldini, L., Brez, A., Latronico, L., Omodei, N., Razzano, M., Massai, M. M., Pesce-Rollins, M., Sgró, C., Costa, E., Soffitta, P., Sipila, H., and Lempinen, E., "A sealed Gas Pixel Detector for X-ray astronomy," *Nuclear Instruments and Methods in Physics Research A* **579**, 853–858 (Sept. 2007).

[7] Feng, H., Jiang, W., Minuti, M., Wu, Q., Jung, A., Yang, D., Citraro, S., Nasimi, H., Yu, J., Jin, G., Huang, J., Zeng, M., An, P., Baldini, L., Bellazzini, R., Brez, A., Latronico, L., Sgrò, C., Spandre, G., Pinchera, M., Muleri, F., Soffitta, P., and Costa, E., "PolarLight: a CubeSat X-ray polarimeter based on the gas pixel detector," *Experimental Astronomy* **47**, 225–243 (Apr. 2019).

[8] Zhang, S., Santangelo, A., Feroci, M., Xu, Y., Lu, F., Chen, Y., Feng, H., Zhang, S., Brandt, S., Hernanz, M., Baldini, L., Bozzo, E., Campana, R., De Rosa, A., Dong, Y., Evangelista, Y., Karas, V., Meidinger, N., Meuris, A., Nand ra, K., Pan, T., Pareschi, G., Orleanski, P., Huang, Q., Schanne, S., Sironi, G., Spiga, D., Svoboda, J., Tagliaferri, G., Tenzer, C., Vacchi, A., Zane, S., Walton, D., Wang, Z., Winter, B., Wu, X., in't Zand, J. J. M., Ahangarianabhari, M., Ambrosi, G., Ambrosino, F., Barbera, M., Basso, S., Bayer, J., Bellazzini, R., Bellutti, P., Bertucci, B., Bertuccio, G., Borghi, G., Cao, X., Cadoux, F., Campana, R., Ceraudo, F., Chen, T., Chen, Y., Chevenez, J., Civitani, M., Cui, W., Cui, W., Dauser, T., Del Monte, E., Di Cosimo, S., Diebold, S., Doroshenko, V., Dovciak, M., Du, Y., Ducci, L., Fan, Q., Favre, Y., Fuschino,

F., Gálvez, J. L., Gao, M., Ge, M., Gevin, O., Grassi, M., Gu, Q., Gu, Y., Han, D., Hong, B., Hu, W., Ji, L., Jia, S., Jiang, W., Kennedy, T., Kreykenbohm, I., Kuvvetli, I., Labanti, C., Latronico, L., Li, G., Li, M., Li, X., Li, W., Li, Z., Limousin, O., Liu, H., Liu, X., Lu, B., Luo, T., Macera, D., Malcovati, P., Martindale, A., Michalska, M., Meng, B., Minuti, M., Morbidini, A., Muleri, F., Paltani, S., Perinati, E., Picciotto, A., Piemonte, C., Qu, J., Rachevski, A., Rashevskaya, I., Rodriguez, J., Schanz, T., Shen, Z., Sheng, L., Song, J., Song, L., Sgro, C., Sun, L., Tan, Y., Uttley, P., Wang, B., Wang, D., Wang, G., Wang, J., Wang, L., Wang, Y., Watts, A. L., Wen, X., Wilms, J., Xiong, S., Yang, J., Yang, S., Yang, Y., Yu, N., Zhang, W., Zampa, G., Zampa, N., Zdziarski, A. A., Zhang, A., Zhang, C., Zhang, F., Zhang, L., Zhang, T., Zhang, Y., Zhang, X., Zhang, Z., Zhao, B., Zheng, S., Zhou, Y., Zorzi, N., and Zwart, J. F., "The enhanced X-ray Timing and Polarimetry mission—eXTP," *Science China Physics, Mechanics, and Astronomy* **62**, 29502 (Feb. 2019).

[9] Peirson, A. L., Romani, R. W., Marshall, H. L., Steiner, J. F., and Baldini, L., "Deep ensemble analysis for Imaging X-ray Polarimetry," *Nuclear Instruments and Methods in Physics Research A* **986**, 164740 (Jan. 2021).

[10] Manfreda, A., "The Gas Pixel Detetcor for the IXPE mission," *Journal of Instrumentation* **15**, C04049 (Apr. 2020).

[11] Weisskopf, M. C., Ramsey, B., O'Dell, S., Tennant, A., Elsner, R., Soffitta, P., Bellazzini, R., Costa, E., Kolodziejczak, J., Kaspi, V., Muleri, F., Marshall, H., Matt, G., and Romani, R., "The Imaging X-ray Polarimetry Explorer (IXPE)," in [Proc. SPIE], *Society of Photo-Optical Instrumentation Engineers (SPIE) Conference Series* **9905**, 990517 (July 2016).

[12] Muleri, F., Lefevre, C., Piazzolla, R., Morbidini, A., Amici, F., Attina, P., Centrone, M., Del Monte, E., Di Cosimo, S., Di Persio, G., Evangelista, Y., Fabiani, S., Ferrazzoli, R., Loffredo, P., Maiolo, L., Maita, F., Primicino, L., Rankin, J., Rubini, A., Santoli, F., Soffitta, P., Tobia, A., Tortosa, A., and Trois, A., "Calibration of the IXPE instrument," in [*Society of Photo-Optical Instrumentation Engineers (SPIE) Conference Series*], **10699**, 106995C (Jul 2018).

[13] Fabiani, S., Muleri, F., Di Marco, A., Monaca, F., Rankin, J., Soffitta, P., Amici, F., Attinà, P., Baldini, L., Barbanera, M., Brienza, D., Castellano, S., Citraro, S., Costa, E., Evangelista, Y., Monte, E., Cosimo, S., Persio, G., Ferrazzoli, R., and Xie, F., "Outcomes of the ixpe instrument calibration," in [Proc. SPIE], *SPIE Astronomical Telescopes + Instrumentation* , 247 (01 2021).

[14] Muleri, F., Piazzolla, R., Di Marco, A., Fabiani, S., La Monaca, F., Lefevre, C., Morbidini, A., Rankin, J., Soffitta, P., Tobia, A., Xie, F., Amici, F., Attinà, P., Bachetti, M., Brienza, D., Centrone, M., Costa, E., Del Monte, E., Di Cosimo, S., Di Persio, G., Evangelista, Y., Ferrazzoli, R., Loffredo, P., Perri, M., Pilia, M., Puccetti, S., Ratheesh, A., Rubini, A., Santoli, F., Scalise, E., and Trois, A., "The ixpe instrument calibration equipment," *Astroparticle Physics* **136**, 102658 (2022).

[15] Rankin, J., Muleri, F., Tennant, A. F., Bachetti, M., Costa, E., Marco, A. D., Fabiani, S., La Monaca, F., Soffitta, P., Tobia, A., Trois, A., Xie, F., Baldini, L., Di Lalla, N., Manfreda, A., O'Dell, S. L., Perri, M., Puccetti, S., Ramsey, B. D., Sgrò, C., and Weisskopf, M. C., "An Algorithm to Calibrate and Correct the Response to Unpolarized Radiation of the X-Ray Polarimeter Onboard IXPE," AJ **163**, 39 (Feb. 2022).

[16] Di Marco, A., Fabiani, S., La Monaca, F., Muleri, F., Rankin, J., Soffitta, P., Xie, F., Amici, F., attinà, P., Bachetti, M., Baldini, L., Barbanera, M., Baumgartner, W., Bellazzini, R., Borotto, F., Brez, A., Brienza, D., Caporale, C., Cardelli, C., Carpentiero, R., Castellano, S., Castronuovo, M., Cavalli, L., Cavazzuti, E., Ceccanti, M., Centrone, M., Citraro, S., Costa, E., D'Alba, E., D'Amico, F., Del Monte, E., Di Cosimo, S., Di Lalla, N., Di Persio, G., Donnarumma, I., Evangelista, Y., Ferrazzoli, R., Latronico, L., Lefevre, C., Loffredo, P., Lorenzi, P., Lucchesi, L., Magazzù, C., Magazzù, G., Maldera, S., Manfreda, A., Mangraviti, E., Marengo, M., Matt, G., Mereu, P., Minuti, M., Morbidini, A., Mosti, F., Nasimi, H., Negri, B., Nuti, A., O'Dell, S. L., Orsini, L., Perri, M., Pesce-Rollins, M., Piazzolla, R., Pieraccini, S., Pilia, M., Pinchera, M., Profeti, A., Puccetti, S., Ramsey, B. D., Ratheesh, A., Rubini, A., Santoli, F., Sarra, P., Scalise, E., Sciortino, A., Sgrò, C., Spandre, G., Tardiola, M., Tennant, A. F., Tobia, A., Trois, A., Vimercati, M., Weisskopf, M. C., Zanetti, D., and Zanetti, F., "Calibration of the IXPE focal plane X-ray polarimeters to polarized radiation," *arXiv e-prints* , arXiv:2206.07582 (June 2022).